PERGAMON

The mechanism of the magnetic interaction in the β phase of the p-(nitro)phenyl nitronyl nitroxide (KAXHAS). A bottom-up study using only ab initio data

Mercè Deumal [a,*], Mike A. Robb [b], Juan J. Novoa [a,*]

[a] *Departament de Química Física and CER Química Teòrica, Universitat de Barcelona, Av. Diagonal 647, E-08028 Barcelona, Spain*
[b] *Department of Chemistry, King's College London, Strand WC2R 2LS, London, UK*

Abstract

The magnetism of the β phase of p-(nitro)phenyl nitronyl nitroxide (KAXHAS) crystal has been studied using a recently developed theoretical approach 'J. Phys. Chem. A 106 (2002) 1299'. This approach is a bottom-up study based on the evaluation of the magnetic interaction between all pairs of radicals (J_{AB}), which allows the definition of the magnetic structure of the crystal. With only such knowledge, one solves an algebraic Heisenberg Hamiltonian on a properly chosen finite subset of the magnetic structure and then computes the magnetic susceptibility $\chi(T)$ and/or heat capacity $C_p(T)$ curves for the crystal. This method is applied here to the KAXHAS crystal. The theoretical $\chi(T)$ and $C_p(T)$ results are in very good agreement with the available experimental data. This theoretical methodology is first reviewed here on physical terms, and then used to rationalize the bulk ferromagnetic behavior of KAXHAS in terms of its corresponding microscopic J_{AB} pair interactions.
© 2003 Elsevier Science Ltd. All rights reserved.

1. Introduction

The rational design of magnetic crystals at a molecular level is still a challenge to theory and experiment [1]. Part of the difficulty in achieving such design is associated with the current limitations to understand the macroscopic magnetic properties of the crystal accurately enough, in order to interpret the macroscopic behavior in terms of microscopic J_{AB} magnetic interactions between adjacent molecules A–B with unpaired spins. If this connection were established, one could search for a properly defined magneto-structural relationship relating the geometrical disposition of the radicals within the crystal and the magnitude of the J_{AB} magnetic interactions, and the rational design could then be achieved. Within this framework, a new computational approach to study the magnetism of

molecular crystals has been recently proposed. This approach rigorously uses the microscopic data on the J_{AB} magnetic interactions computed using ab initio methods to evaluate the macroscopic magnetic properties of the crystal [2], such as magnetic susceptibility $\chi(T)$ and heat capacity $C_p(T)$.

In this paper, we first review the methodology presented in theoretical terms in Ref. [2]. We will present it in physical terms. Then we will illustrate its usage and potentiality by carrying out an in-depth analysis of the magnetism of the β phase of the *para*-(nitro)phenyl nitronyl nitroxide radical (the β-p-(NO₂)PhNN [3] crystal, or KAXHAS according to the Cambridge Structural Database convention [4], see Scheme 1). KAXHAS is selected for being the first purely organic crystal reported to have bulk ferromagnetic properties. Although various studies have been carried out before to understand its bulk magnetic properties [3,5], none of them was done at the level of accuracy and detail of the analysis presented here. Such analysis will also illustrate

---

* Corresponding authors.
E-mail addresses: m.deumal@qf.ub.es (M. Deumal), mike.robb@kcl.ac.uk (M.A. Robb), novoa@qf.ub.es (J.J. Novoa).
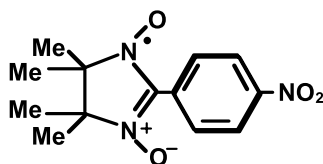
Scheme 1.

the capabilities of the theoretical methodology used here [2].

The bottom-up method used here to rationalize the magnetic properties of molecular crystals rigorously computes the *macroscopic* magnetic properties of KAX-HAS from the only knowledge of the non-redundant *microscopic* magnetic interactions between all different A–B radical-pairs present in the crystal (J_{AB}). Once all unique J_{AB} pair interactions in the crystal are determined, one can define the magnetic structure for that crystal as a graphical representation of all possible magnetic pathways along which the dominant magnetic interactions can propagate within the crystal. Thus, the magnetic structure depicts the topology of the computed J_{AB} magnetic interactions between the constituent radicals in the crystal. From that magnetic structure, one can define a minimal finite-size model where all J_{AB} interactions preserve the same environment they have in the infinite crystal. This minimal magnetic model is then used to solve the secular equation problem of an algebraic Heisenberg Hamiltonian. It is worth stressing the fact that this is the first time a Heisenberg Hamiltonian with realistic coupling parameters has been used to study magnetism [2]. The macroscopic magnetic susceptibility $\chi(T)$ (or heat capacity $C_p(T)$) is, in turn, obtained directly from the computed energy levels of the algebraic Heisenberg Hamiltonian using standard statistical mechanics. For any given molecular crystal, one can relate macroscopic magnetic properties to microscopic J_{AB} magnetic interactions by using this procedure, thus allowing a rational and unbiased analysis of the magnetism of that crystal.

KAXHAS crystallizes into the orthorhombic *F2dd* space group ($a = 12.347$ Å, $b = 19.364$ Å, $c = 10.971$ Å) with eight radicals per unit cell. The experimental magnetic susceptibility data for this crystal was fitted to the Curie–Weiss expression Eq. (1) with $\theta = +1.2$ K ($+0.84$ cm^{-1}) and $C = 0.376$ emu K mol^{-1} in the temperature range between 4 and 300 K [3]. For a ferromagnet (FM), such as KAXHAS, the Curie–Weiss model [6] is often used to fit the experimental magnetic susceptibility data. This model focuses on the transition between two doublet radical states with spin $-1/2$ and $1/2$, and predicts the susceptibility to be

$$\chi = \frac{C}{(T - \theta)} \quad \text{(emu mol}^{-1}\text{)} \tag{1}$$

where C is the Curie constant

$$C = \frac{Ng^2\mu_B^2 S(S + 1)}{3k_B} \tag{2}$$

and θ is the Weiss temperature

$$\theta = \frac{zJS(S + 1)}{3k_B} \tag{3}$$

In the Curie–Weiss model each radical center interacts with z nearest neighbors with a dimeric interaction J. As the model embodied in Eq. (1) is phenomenological, the J parameter obtained from a fitting procedure does not represent a real microscopic pair interaction J_{AB}. Rather, as an organic molecular solid must have many different dimeric interactions J_{AB} between constituent A–B radicals, the observed J in Eq. (3) can be taken as an effective parameter resulting from a complicated interplay of all J_{AB} values. Furthermore, even if the fitting itself is numerically appropriate, the physical model embodied in Curie–Weiss Eq. (1) is often not adequate to interpret the real magnetic behavior for a given crystal.

In this paper, we will illustrate how the above described method [2] works by rationalizing the bulk ferromagnetism of the β-*p*-(NO$_2$)PhNN (KAXHAS) crystal. We will show that the bulk ferromagnetism in KAXHAS is properly reproduced by only using two types of FM pair interactions J_{AB}. However, this simplicity is only apparent. Once all the important J_{AB} pair interactions are known, the topology of these pairs (i.e. the magnetic structure) is crucial to determine the macroscopic magnetic properties of the crystal. We will thus show that in KAXHAS the two FM J_{AB} pair interactions present a very complex three-dimensional topology.

2. Computational details

The theoretical, mathematical and physical foundations of the procedure we use to study the magnetism in molecular crystals has been already described [2]. Therefore, here they will only be reviewed from a physical perspective. Such a computational approach is based on the following steps: (1) analysis of the crystal packing to identify all potentially relevant magnetic pair A–B interactions, (2) ab initio computation of the J_{AB} value for all selected magnetic interactions, (3) definition of the magnetic structure of the crystal and the corresponding minimal finite-size model system used to solve the algebraic Heisenberg Hamiltonian secular equation problem, and (4) simulation of the magnetic susceptibility $\chi(T)$ via statistical mechanics using the computed microscopic energy levels of the minimal magnetic model defined in Eq. (3). We will next present the most important details for each step.

First of all, we aim to select all unique A−B radical-pairs within the crystal in an unbiased way (step 1). A detailed analysis of the crystal packing is carried out, without assuming any preconceived microscopic magnetic exchange path. It consists of selecting all possible different A−B radical-pairs within the crystal according to a given cutoff distance between their spin carriers. This cutoff criterion results from the fact that the magnetic interaction is known to decrease exponentially according to the distance r between magnetic centers and to depend on the relative orientation of constituent radicals [7]. Notice that the distance criterion per se does not determine the relevant magnetic exchange pathways. Rather, it provides the initial pairs of radicals A−B for the subsequent computation of the J_{AB} values. We deliberately select the cutoff in order to include in the list of candidate pairs more than the first nearest neighbors to a given radical A, which are the usual candidates in the literature. KAXHAS (see Scheme 1) has just one unpaired electron that is mostly delocalized on the ONCNO atoms, which are thus taken as the 'spin carrier group'. We have then selected as candidate A−B pairs, all those pairs whose ONCNO···ONCNO distance is shorter than 7.4 Å [7] (these pairs will be identified as d_i).

The value of the J_{AB} pair interaction (step 2) is then computed for all candidate A−B pairs d_i, using the X-ray geometry of both radicals. The objective of this step is to discriminate whether these pair interactions are magnetically important or not. For organic crystals, a 'bare' dimer approach is adequate enough. For each pair of radicals A−B with one $S = 1/2$ unpaired electron in KAXHAS, the J_{AB} value has been simply computed as the singlet–triplet S–T energy separation using unrestricted DFT with broken symmetry (BS) approach [8], since the solutions for the biradical open-shell singlet were localized SOMOs on one radical or on the other and so the SOMOs overlap is negligible ($S_{ab} = 0$) (see Ref. [2] for a more detailed discussion). The computation of J_{AB} values has been carried out using the UB3LYP functional [9] with a 6−31+G(d) basis set [10] (GAUSSIAN package [11]). Notice that the only possible sources of error in the evaluation of the J_{AB} value should be associated to the use of the UB3LYP-BS method (UB3LYP-BS results have 10–15% systematic error compared to FCI, MCSCF or similar methods), and to the collective role played by nearby radicals, which is neglected by a dimer approach.

Once the non-negligible J_{AB} pair interactions are known, the magnetic structure of the crystal can be defined (step 3). The magnetic structure describes how the constituent radicals are magnetically inter-connected within the crystal by means of the J_{AB} magnetic pair interactions. Accordingly, it is a topological map of the magnetic interactions. We thus picture the topology of the magnetic structure in terms of the magnitude of J_{AB}

interactions using geometrical keywords such as zigzag *chains*, spin *ladders*, alternant *layers*, etc. By definition, such a pictorial representation contains all important magnetic pathways, along which the magnetic interaction can propagate within the crystal.

The simulation of macroscopic magnetic properties from microscopic data is carried out using statistical mechanics [12]. Within this framework, the magnetic susceptibility $\chi(T)$ is then defined as

$$\chi = \frac{N_A g^2 \mu_B^2}{3 k_B T} \mu_0 \left[\frac{\sum_n S_n(S_n + 1)(2S_n + 1) \exp\left[-\dfrac{E_n - E_0}{k_B T}\right]}{\sum_n (2S_n + 1) \exp\left[-\dfrac{E_n - E_0}{k_B T}\right]} \right]$$

(4)

and the heat capacity $C_p(T)$ as

$$C_p = \frac{N_A}{k_B T^2} \left[\frac{\sum_n (2S_n + 1)(E_n - E_0)^2 \exp\left[-\dfrac{E_n - E_0}{k_B T}\right]}{\sum_n (2S_n + 1) \exp\left[-\dfrac{E_n - E_0}{k_B T}\right]} \right.$$
$$\left. - \frac{\left(\sum_n (2S_n + 1)(E_n - E_0) \exp\left[-\dfrac{E_n - E_0}{k_B T}\right]\right)^2}{\left(\sum_n (2S_n + 1) \exp\left[-\dfrac{E_n - E_0}{k_B T}\right]\right)^2} \right]$$

(5)

using the microscopic energy levels E_n obtained from the diagonalization of an algebraic Heisenberg Hamiltonian

$$\hat{H} = -\sum_{A,B}^{N} J_{AB} \left(2\hat{S}_A \hat{S}_B + \frac{1}{2} \hat{I}_{AB} \right)$$

(6)

which is parameterized with the previously computed J_{AB} (step 2) and where $\hat{S}_A$ is the spin operator associated with the radical A, and $\hat{I}_{AB}$ is the identity operator. The sum over A and B runs over a set of N magnetic $S = 1/2$ centers or sites, on the understanding that there is a one-to-one correspondence between radical molecule and magnetic site. In Eqs. (4) and (5), E_n is the n-th energy level from the algebraic Heisenberg Hamiltonian Eq. (6), S_n is the spin of the n-th energy level, g is the gyromagnetic factor, and the constants N_A, μ_B, k_B and μ_0 are Avogadro's number, Bohr magneton, Boltzmann constant, and permeability of free space, respectively.

In principle, the number N of magnetic $S = 1/2$ centers in Eq. (6) is infinite, since a real crystal is made of an infinite number of radical molecules. However, in order to diagonalize the Heisenberg Hamiltonian Eq. (6), one must reduce the problem from an infinite crystal to a finite model using the periodicity of

the magnetic structure. Good candidates for such a finite-size model are any subset of N magnetic centers containing all relevant magnetic J_{AB} interactions and presenting the same topological connectivity that these interactions have in the magnetic structure of the infinite crystal. The smallest of such subsets is called *minimal magnetic model space*, and is the model used for the numerical solution of Eq. (6). From a crystallographic point of view, a natural choice for the minimal magnetic model space would be the crystallographic unit cell. However, a simple example can illustrate that the selection of the N number of magnetic centers must be carried out according to the topology of the magnetic structure, and not according to the repetition of crystallographic cells of the crystal. Scheme 2 shows the topology of a two-dimensional layer in terms of pair interactions J_1, J_2, and J_3. For instance, assuming $J_3 \ll J_1, J_2$, the magnetic structure shown in Scheme 2 is an array of non-interacting spin ladders with rungs given by J_1 and legs by J_2. In such a case, a spin ladder is the magnetic motif providing all the relevant microscopic information, and the corresponding minimal magnetic model will require four radical centers with two J_1 and two J_2 interactions, as shown inset in Scheme 2 [13]. In contrast, the broken lines in Scheme 2 represent a crystallographic unit cell containing two pairs of radicals A and B connected by the microscopic magnetic interactions J_2 and J_3. It follows that the repetition of this unit cell cannot possibly generate the magnetic structure (i.e. spin ladder) of Scheme 2 since the J_3 interaction is taken to be negligible compared to J_1 and J_2 pair interactions. One can thus conclude that there is no reason to choose the crystallographic unit cell as minimal magnetic model. In fact, the minimal magnetic model space is the minimal set of pair interactions J_{AB}'s whose repetition along the three crystallographic directions generates the actual crystal magnetic structure and whose simulated macroscopic magnetic data reproduces qualitatively the experimental data. If the chosen minimal magnetic model is correct, enlarging its size only increases the dimensionality N of the matrix representation of the Heisenberg Hamiltonian Eq. (6) and, thus the
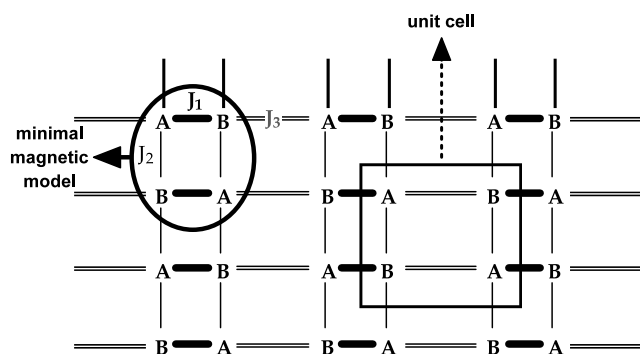
computational cost. However, it does not change the quality of the computed magnetic properties. In practice, the set of N magnetic $S = 1/2$ centers that defines the minimal magnetic model are often simple geometric sub-structures such as *chains*, *ladders*, but more complicated three-dimensional structures can also be encountered. Therefore, the selection of the *minimal magnetic model space* is a crucial step in the computational procedure [2].

Once the minimal magnetic model space has been selected and the secular equation problem (Eq. (6)) solved, the magnetic susceptibility and heat capacity can be finally computed and compared to experimental data (according to Eqs. (4) and (5), respectively) (step 4). Notice that whenever we talk in the paper about *experimental* $\chi(T)$ data we refer to experimentally fitted data not raw data since most of the experimental papers give expressions with which to fit the raw $\chi(T)$ data but not the raw $\chi(T)$ data itself.

3. Results and discussion

From a crystallographic point of view, the KAXHAS crystal [3] is formed by two types of *ac* planes of radical molecules, A and B, which pile up along the *b* axis according to an ABABA sequence (see Fig. 1, inset *a*, *b*, *c* axes are given). The overall geometrical arrangement of the radicals follows a tetrahedral disposition with
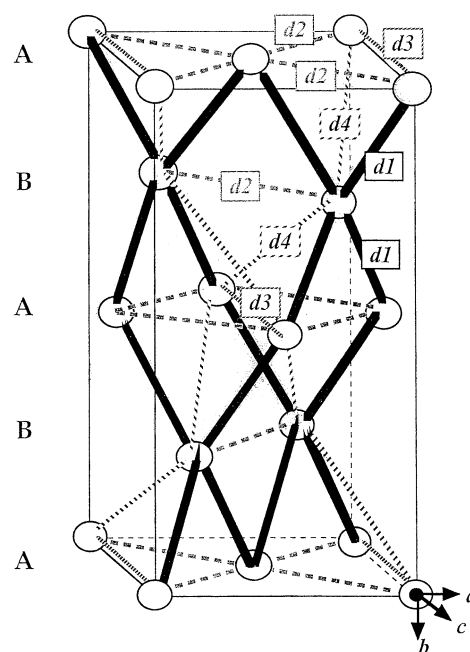

Fig. 1. Dimeric interactions (d_1–d_4) resulting from the analysis of the crystal packing for KAXHAS in terms of O···O distance between ONCNO groups being shorter than 7.4 Å. The O···O distance for all interactions is given in Table 1.

Scheme 2.

three corners of the tetrahedron in one plane and the remaining one in any of the nearby planes.

According to the previously described 4-step prescription, we start the discussion on the magnetism of KAXHAS by analyzing the crystal packing in terms of intermolecular $O \cdots O$ distances between ONCNO groups shorter than 7.4 Å [7], as these are the groups where most of the spin density is located on the *p*-nitrophenyl nitronyl nitroxide [14]. This analysis suggests four different non-redundant pairs of radicals, $d_i = d_1 - d_4$, whose $J_{AB}(d_i)$ dimeric interaction should then be computed in order to discriminate whether a given d_i is magnetically important or not (see Fig. 1 for $d_1 - d_4$ within a unit cell).

The $J_{AB}(d_i)$ values for the $d_1 - d_4$ pairs are then computed using the unrestricted DFT BS approach. The results using the UB3LYP functional and $6-31+$ G(d) basis set for the four d_i candidates of KAXHAS are given in Table 1 ($d_1 - d_4$ listed as $O \cdots O$ distance increases). Table 1 shows that only two pair interactions (J_1 and J_2) are magnetically important and will contribute to the macroscopic magnetism of the crystal. Notice that both microscopic pair interactions are ferromagnetic. Once more, resorting to the ABABA crystallographic description of the crystal, one would say that the interplane J_1 pair interaction is more than three times stronger than the intraplane J_2 pair interaction. This result is consistent with what Kinoshita [3c] suggested from the analysis of KAXHAS crystal structure: at least, two kinds of exchange interactions (J out-of-plane and J' in-plane) were expected to dominate the ferromagnetism of KAXHAS. It also agrees with the APUHF INDO computations carried out by Okumura et al. [5], who estimated these interactions to be $J = +$ 0.17 cm^{-1} and $J' = +0.08$ cm^{-1}. Our computed values obtained at UB3LYP/6$-31+$G(d) level are $J_1 = +0.62$ cm^{-1} and $J_2 = +0.18$ cm^{-1} to be compared to J and J' [5], respectively. There is a clear difference between these values as a consequence of a better description of the energy at the DFT level. However, the important point here is that both studies reach the same qualitative conclusion about which exchange interactions J_1, J_2 are magnetically important.

Table 1
Unrestricted DFT BS UB3LYP/6$-31+$G(d) results for the dimeric interaction of all four candidates ($d_1 - d_4$ listed as $O \cdots O$ distance increases) for KAXHAS

Candidate d_i	$d_i(O \cdots O)$ (Å)	J_i (cm^{-1})	J_i ordering
d_1	5.35	+0.62	J_1
d_2	6.43	+0.18	J_2
d_3	6.73	< |0.05|	
d_4	6.90	< |0.05|	

The fourth column gives the ordering of the non-negligible dimeric interactions J_1, J_2 from strongest to weakest dimeric interaction.
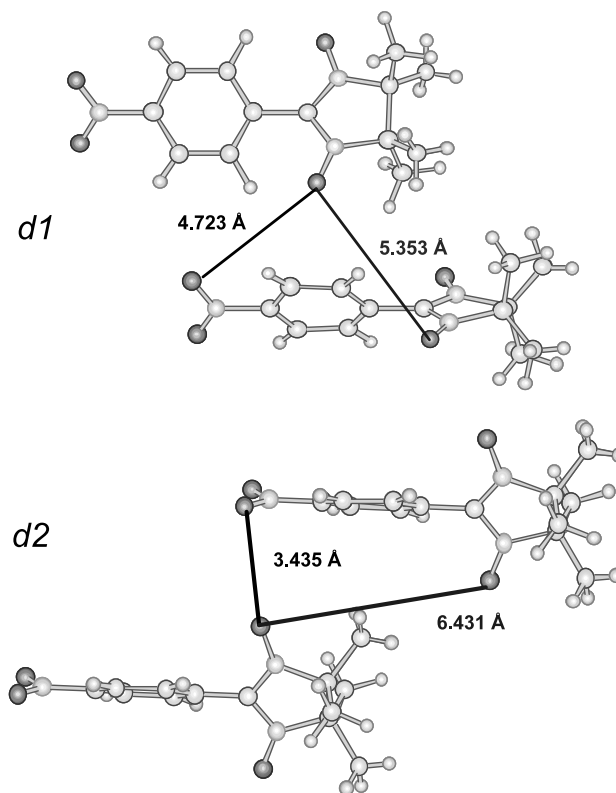

Fig. 2. Geometry of the d_1 and d_2 pairs associated to the J_1, J_2 magnetic interactions.

Fig. 2 shows the geometry of the dimers associated to the J_1 and J_2 pair interactions, indicating the main $O \cdots$ O distances. It is interesting to stress that none of these two pairs obey the McConnell-I mechanism, as there are no short contacts between the atoms of the ONCNO groups (the distances are too large). The magnetic interaction has been sometimes considered to take place through the O atoms of the NO_2 group, but these groups have a very small atomic spin population on them, similar to that found on the H atoms of the six-membered ring. So, if one were to consider a ONCNO $\cdots NO_2$ interaction, one should also consider a ONCNO $\cdots HC$ interaction. However, the fact that a larger ONCNO $\cdots NO_2$ contact (in J_1) gives rise to a stronger magnetic interaction than a shorter one (in J_2) goes against the fact that magnetic interactions are driven by a ONCNO $\cdots NO_2$ interaction, that is, it rules out the validity of the McConnell-I proposal to rationalize the magnetic interaction in the KAXHAS crystal. This is not surprising, as the McConnell-I proposal was shown to lack of the adequate theoretical foundations and work only when a high symmetry situation is encountered (e.g. paracyclophanes [15]). It even fails to predict the magnetism of simple NO containing dimers [16]. Thus, one should avoid analyzing the nature of the magnetic interactions using a model whose validity has been demonstrated to fail in many cases.
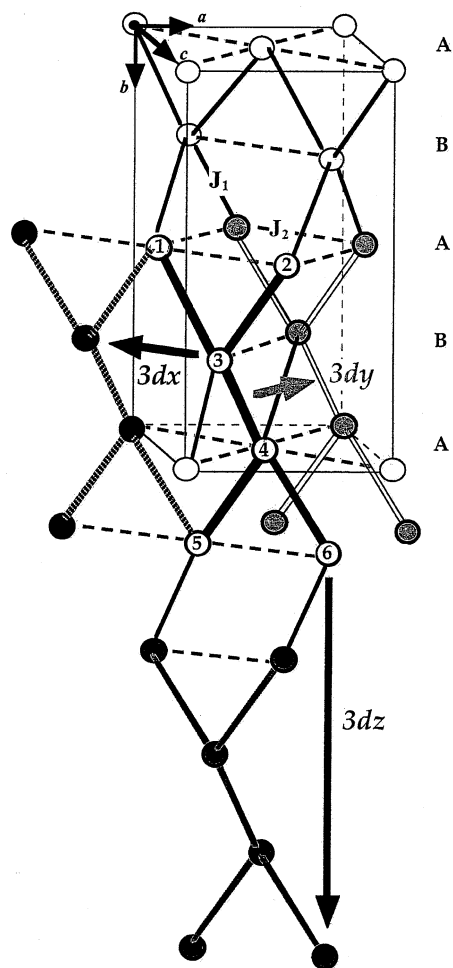
Fig. 3. Non-negligible J_1, J_2 magnetic interactions between radicals in terms of KAXHAS crystallographic cells (each radical is replaced by a point site, for formula see Scheme 1). According to J_2 (broken lines), the radicals pack forming ABABA planes (*ac* crystallographic directions) as shown in the upper right unit cell. According to J_1 (thick lines), the magnetic structure (and so the minimal magnetic model) is three-dimensional. The *6s_3d* magnetic repeating unit is given with point sites labeled 1–6. Inset in the figure, the propagation of the *6s_3d* model required to fill the three-dimensional magnetic structure along the *b* axis (*3dz*) and *a/c* axes (*3dx* and *3dy*) is shown.

Fig. 3 shows the magnetic structure for KAXHAS. Notice that each radical molecule is replaced by a point site (see Scheme 1 for radical formula). The magnetic structure is clearly three-dimensional and ferromagnetic along all directions, which is consistent with KAXHAS being experimentally a bulk FM.

One should next proceed by identifying the minimal magnetic model defined by the dominant J_{AB} interactions. Thus, one must identify the smallest repeating unit required to generate the magnetic structure of KAXHAS by propagating a subset of J_1 and J_2 magnetic interactions along all spatial directions. For KAXHAS, we found that a six-magnetic site, three-dimensional model (point sites labeled 1–6 in Fig. 3) is a suitable repeating unit, i.e. the minimal magnetic model (which

we shall call *6s_3d*). In Fig. 3 we show how the propagation (i.e. extension along *a, b, c* axes) of the *6s_3d* model generates the three-dimensional magnetic structure. There is a *pure* translation along the *b* crystallographic axis (*3dz*, 12-site model) and two *mixed* translations along combinations of *a/c* axes (*3dx*, 10-site model and *3dy*, 12-site model). Notice that KAXHAS crystallographic unit cells are explicitly pictured in Fig. 3 to indicate that the selection of the minimal magnetic model and its extension does not depend on the unit cell per se but on the symmetry of the magnetic structure itself.

For KAXHAS, the minimal *6s_3d* magnetic model is then used for diagonalization of the algebraic Heisenberg Hamiltonian (Eq. (6)) to compute the microscopic energy levels (Fig. 4(a)) required by the statistical mechanics definition of the magnetic susceptibility and heat capacity (Eqs. (4) and (5), respectively). Fig. 5 shows the computed magnetic susceptibility using the minimal *6s_3d* model, which reproduces very well the experimental data available. Convergence on the magnetic susceptibility $\chi(T)$ has been also explored by extending the six-site three-dimensional (*6s_3d*) model along *a*, *b* and *c* crystallographic directions (see Fig. 3 for *3dx*, *3dy* and *3dz* models, and Fig. 4(b and c) for microscopic energy levels). Fig. 5 shows that all simulated results for $\chi(T)$ converge at high and low temperatures, where $\chi T(T)$ is plotted in order to appreciate better the comparison among simulated data. Thus, the *6s_3d* model is adequate to represent the magnetic structure for KAXHAS. We are left now with addressing the difference between experimental and simulated $\chi(T)$ data. The minimal *6s_3d* magnetic model for KAXHAS requires a scaling factor of 1.8 applied to its J_{AB} values to reproduce the experimental $\chi(T)$ data (the substituent attached to the α-C of the NN group is a phenyl group and so the cooperative effects will be non-negligible) [17].

At this point, it is worth comparing the value of the computed J_{AB} pair interactions against the value one would obtain for the effective parameter J (using Eq. (3)) estimated from the empirical Curie–Weiss fitting (Eq. (1)) to the experimental magnetic susceptibility data. Let us remind the reader that according to this model, a given magnetic center interacts with strength J (mean intermolecular interaction) with a number z of nearest neighbor centers in the crystal lattice [6,18]. We first need to determine the number z of nearest neighbors. From Fig. 3 one can see that each magnetic (radical) center interacts through J_1 with four nearest neighbors and through J_2 with other four; z being either four or eight, respectively. Using Eq. (3), $J(z=4)$ is + 0.83 cm^{-1} and $J(z=8)$ is +0.42 cm^{-1}. Comparing these values to $J_1(+0.62$ cm$^{-1})$ and $J_2(+0.18$ cm$^{-1})$, we realize that $J(z=4)$ is too large because it does not account for J_2-type interactions and $J(z=8)$ is too small

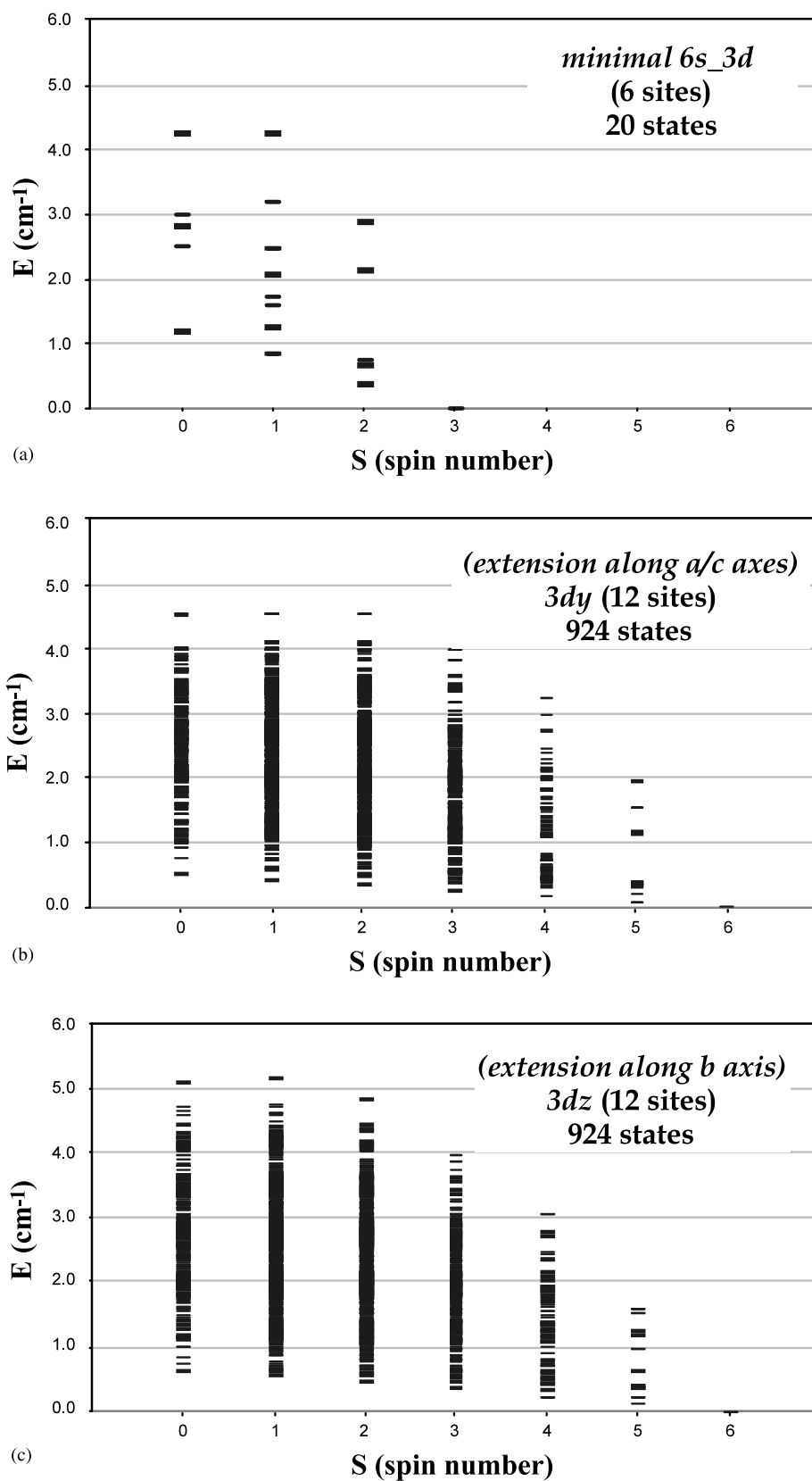Fig. 4. Energy spectra vs. spin number for (a) minimal *3d_6s*, (b) *3dy* and (c) *3dz* models. Inset the number of sites is given. The number of energy levels increases with the *N* number of unpaired electrons as $[N!/(N/2)!*(N/2)!]$. The limiting values of the spin number are $S = 0$ and $S = N*(1/2)$.
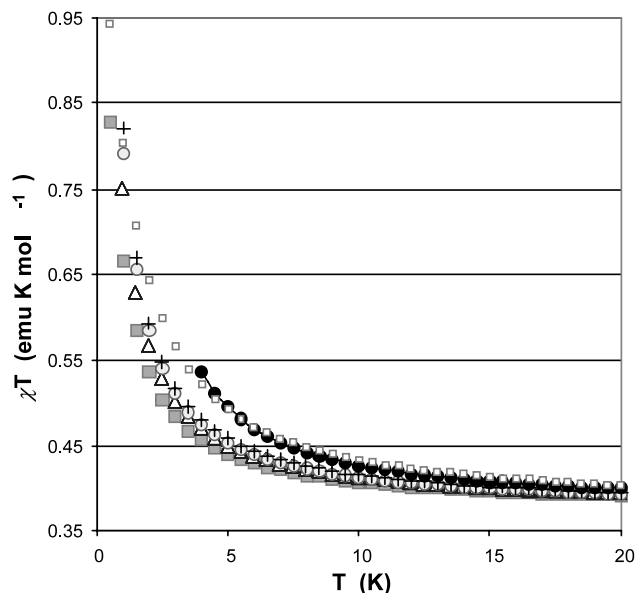
Fig. 5. Simulated results for $\chi T(T)$ using the *6s_3d* model (▨) and its extension *3dx* (△), *3dy* (○), and *3dz* (+). A scaling factor of 1.8 applied to the *6s_3d* minimal model (ρ) is required to reproduce the experimental $\chi(T)$ data (●).

since it does not distinguish between J_1 and J_2 interactions. Therefore, a Curie–Weiss expression Eq. (1) has limited value for understanding the microscopic picture of a magnetic center interacting with its neighbors due to the fact that this methodology averages all magnetic interactions. Besides, expression Eq. (1) is a modification of the Curie law to account for weak intermolecular interactions among radicals with non-accessible excited states (large separation between ground and first excited states) and no first order angular momentum (for discussion see Refs. [6,18]). Here, we must stress that the energy spectra for KAXHAS using any of the magnetic models in Fig. 3 (*6s_3d*, *3dx*, *3dy* and *3dz*) shows that all the energy levels are accessible (see Fig. 4), not just the ground state, as assumed in the derivation of the Curie–Weiss expression. It follows that for a FM, such as KAXHAS, there is no reason for the application of the one-level Curie–Weiss model. The fact that such a model empirically fits the experimental magnetic susceptibility for KAXHAS is not a valid argument to justify the use of the Curie–Weiss expression Eq. (1) to interpret the ferromagnetism of KAXHAS.

Finally, we have also simulated the heat capacity $C_p(T)$ data for KAXHAS by using the *6s_3d* minimal model and extending it along a, b and c crystallographic directions (see Fig. 3 for *3dx*, *3dy* and *3dz* models). Statistical mechanics provides an expression for $C_p(T)$ (Eq. (5)) in terms of microscopic energy levels (the units for C_p are J mol^{-1} K^{-1}). The experimental heat capacity has a sharp peak at the ferromagnetic transition temperature T_c of 0.6 K, corresponding to a three-

dimensional (second order) magnetic phase transition. Fig. 6 shows the simulated $C_p(T)$ data for KAXHAS. The maximum temperature for all models gives a critical temperature of 0.45 K, which is in good qualitative agreement with the experimental ferromagnetic transition temperature. Notice that Fig. 6 does not show the typical λ-shape of $C_p(T)$ since we are not using the infinite crystal but a small finite model. However, one can see that when increasing the number of magnetic centers in the model from six (minimal *6s_3d* model) to 12 (*3dy* and *3dz* models) the curve does get closer to a λ-shape.

4. Conclusions

The method we have used in this work to study the magnetism in molecular crystals has been shown to reproduce the experimental data (magnetic susceptibility $\chi(T)$, heat capacity $C_p(T)$ and ferromagnetic ordering temperature), as well as rationalize the bulk ferromagnetism of KAXHAS. We have thus shown that we can directly relate the microscopic magnetic information (magnetic structure/topology defined by J_{AB} pair interactions) to the macroscopic properties of a crystal (e.g. magnetic susceptibility, heat capacity, etc.). There are no empirical parameters, as the only input data required is the value of J_{AB} interactions, which is computed using ab initio methods (e.g. DFT). The computation of J_{AB} interactions takes explicitly into account the dependence of the magnetic interaction on the distance and relative orientation of the radical-pairs. For the KAXHAS crystal, only two J_{AB} pair interactions matter, both of them being ferromagnetic with values $+0.62$ and $+0.18$ cm^{-1}. The topology of the three-dimensional magnetic structure generated by these two microscopic J_{AB} pair interactions is consistent with KAXHAS being a bulk FM.

Our computations also suggest that the Curie–Weiss model only provides a mechanism for fitting the experimental magnetic susceptibility data for KAXHAS. It cannot provide understanding about the microscopic picture of the interacting magnetic centers (i.e. J_{AB}) nor about the energy spectrum, which shows an almost continuum of levels. Moreover, we must stress here that the J value obtained from the Curie–Weiss fitting must not be taken as a J_{AB} microscopic magnetic interaction. It is instead an average parameter of all the relevant microscopic magnetic interactions within a given crystal.

Acknowledgements
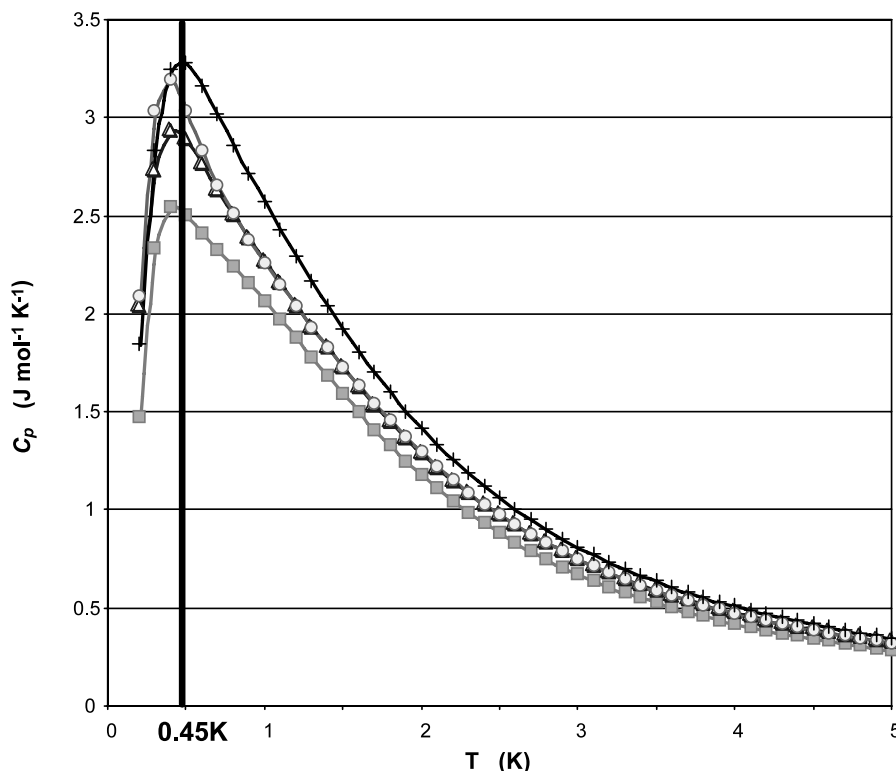
Fig. 6. Simulated $C_p(T)$ data for KAXHAS using the *6s_3d* minimal model (▨) and its extension *3dx* (△), *3dy* (○), and *3dz* (+).

References

[1] (a) All the Proceedings of the International Conference on Molecule-Based Magnets, the latest being: Proceedings of the Fourth International Conference on Molecule-based Magnets, Polyhedron 20 (2001) 1115–1784;
(b) Molecular Magnetism: From Molecular Assemblies to the Devices; in: E. Coronado, P. Delhaès, D. Gatteschi, J.S. Miller (Eds.), NATO Advanced Study Institute Series E321, Kluwer Academic Publishers, Dordrecht, 1996;
(c) O. Kahn, Molecular Magnetism, VCH, New York, 1993.

[2] M. Deumal, M.J. Bearpark, J.J. Novoa, M.A. Robb, J. Phys. Chem. A 106 (2002) 1299.

[3] (a) M. Tamura, Y. Nakazawa, D. Shiomi, K. Nozawa, Y. Hosokoshi, M. Ishikawa, M. Takahashi, M. Kinoshita, Chem. Phys. Lett. 186 (1991) 401;
(b) Y. Nakazawa, M. Tamura, N. Shirakawa, D. Shiomi, M. Takahashi, M. Kinoshita, M. Ishikawa, Phys. Rev. B 46 (1992) 8906;
(c) M. Kinoshita, Jpn J. Appl. Phys. 33 (1994) 5718.

[4] KAXHAS, refcode according to Cambridge Crystallographic Database (CCDC): (a) F.H. Allen, J.E. Davies, J.J. Galloy, O. Johnson, O. Kennard, C.F. Macrae, D.G. Watson, J. Chem. Inf. Comput. Sci. 31(1991) 204;
(b) F.H. Allen, O. Kennard, Chem. Des. Automat. News 8 (1993) 31.

[5] M. Okumura, W. Mori, K. Yamaguchi, Mol. Cryst. Liq. Cryst. 232 (1993) 35.

[6] For discussion on Curie–Weiss law, see references: (a) O. Kahn, Molecular Magnetism, VCH Publishers, New York, 1993, p. 26;
(b) R. Boca, Theoretical Foundations of Molecular Magnetism; Current Methods in Inorganic Chemistry, vol. 1, Elsevier Science, Amsterdam, 1999, p. 53.

[7] (a) C. Herring, Direct exchange between well-separated atoms, in: G.T. Rado, H. Suhl (Eds.), Magnetism, vol. IIB, Academic Press, New York, 1966, p. 5;
(b) For nitronyl nitroxide NN crystals, a spin carrier intersite threshold ONCNO···ONCNO distance of 7.4 Å is chosen to ensure the identification of all potentially important magnetic interactions. This threshold distance comes from increasing by 1.00 Å the largest ONCNO···ONCNO distance between radicals (6.43 Å for KAXHAS) with a non-negligible magnetic J_{AB} interaction computed so far. For crystal and magnetic data, see Ref. [1].

[8] For a discussion on unrestricted DFT with broken symmetry, see:
(a) L. Noodlemann, J. Chem. Phys. 74 (1981) 5737;
(b) L. Noodlemann, E.R. Davidson, Chem. Phys. 109 (1986) 131;
(c) R.G. Parr, W. Yang, Density-Functional Theory of Atoms and Molecules, Oxford University Press, New York, 1989;
(d) L. Noodlemann, D.A. Case, Adv. Inorg. Chem. 38 (1992) 423;
(e) L. Noodlemann, C.Y. Peng, D.A. Case, J.M. Mouesca, Coord. Chem. Rev. 144 (1995) 199;
(f) E. Ruiz, P. Alemany, S. Alvarez, J. Cano, J. Am. Chem. Soc. 119 (1997) 1297;
(g) R. Caballol, O. Castell, F. Illas, .D.R. Moreirai, J.P. Malrieu,

J. Chem. Phys. A, 101 (1997) 7860;
(h) E. Ruiz, J. Cano, S. Alvarez, P. Alemany, J. Comput. Chem. 20 (1999) 1391;
(i) H. Nagao, M. Nishino, Y. Shigeta, T. Soda, Y. Kitagawa, T. Onishi, Y. Yoshioka, K. Yamaguchi, Coord. Chem. Rev. 198 (2000) 265;
(j) J.-M. Mouesca, J. Chem. Phys. 113 (2000) 10505;
(k) F. Illas, D.R. Moreirai, C. de Graaf, V. Barone, Theor. Chem. Acc. 104 (2000) 265.

[9] (a) A.D. Becke, Phys. Rev. A 38 (1988) 3098;
(b) C. Lee, W. Yang, R.G. Parr, Phys. Rev. B 37 (1988) 785;
(c) A.D. Becke, J. Chem. Phys. 98 (1993) 5648.

[10] $6-31+G(d) \equiv DZ$ basis set including diffuse and polarization functions.

[11] M.J. Frisch, G.W. Trucks, H.B. Schlegel, P.M.W. Gill, B.G. Johnson, M.A. Robb, J.R. Cheeseman, T. Keith, G.A. Petersson, J.A. Montgomery, K. Raghavachari, M.A. Al-Laham, V.G. Zakrzewski, J.V. Ortiz, J.B. Foresman, J. Cioslowski, B.B. Stefanov, A. Nanayakkara, M. Challacombe, C.Y. Peng, P.Y. Ayala, W. Chen, M.W. Wong, J.L. Andres, E.S. Replogle, R. Gomperts, R.L. Martin, D.J. Fox, J.S. Binkley, D.J. Defrees, J. Baker, J.P. Stewart, M. Head-Gordon, C. Gonzalez, J.A. Pople, GAUSSIAN 98, Gaussian Inc., Pittsburgh, PA, 1999.

[12] Experimentally, susceptibility measurements are conducted at very low magnetic fields to avoid saturation effects in the magnetic data (e.g. using a SQUID magnetometer). Thus, the expression for $\chi(T)$ (Eq. (4)) has been derived at zero magnetic field B limit. For more information, see: (a) R.L. Carlin, Magnetochemistry, 1986, Springer, Berlin;

(b) R. Boca, Theoretical Foundations of Molecular Magnetism; Current Methods in Inorganic Chemistry, vol. 1, 1999, Elsevier Science, Amsterdam.

[13] For examples, see WILVIW and TOLKEK crystals in Ref. [2].

[14] Ab initio calculations on a family of nitronyl nitroxides have shown that the spin density is mostly localized on the ONCNO group: (a) M. Deumal, P. Lafuente, F. Mota, J.J. Novoa, Syn. Met. 122 (2001) 477;
In the case of the p-nitro-phenyl nitronyl nitroxide, a Mulliken population anaylsis of the UB3LYP/$6-31+G(2d,2p)$ wavefunction shows that the population on the O, N and C atoms of the ONCNO group are 0.33, 0.29 and -0.15 electrons, while those on the N and O atoms of the NO_2 group are 0.002 and -0.003 electron

[15] (a) H.M. McConnell, J. Chem. Phys. 39 (1963) 1910;
(b) M. Deumal, J.J. Novoa, M.J. Bearpark, P. Celani, M. Olivucci, M.A. Robb, J. Phys. Chem. A 102 (1998) 8404.

[16] J.J. Novoa, M. Deumal, P. Lafuente, M.A. Robb, Mol. Cryst. Liq. Cryst. 335 (1999) 603.

[17] Notice that, although a simple linear scaling has been adequate to reproduce qualitatively the experimental $\chi(T)$ data, we could refine the microscopic J_{AB} values using a general non-linear fitting to the actual experimental $\chi(T)$ data.

[18] For mean field theory, see references: (a) O. Kahn, Molecular Magnetism, VCH Publishers, New York, 1993, pp. 26–131;
(b) R.L. Carlin, Magnetochemistry, Springer, Berlin, 1986, p. 113;
(c) R. Boca, Theoretical Foundations of Molecular Magnetism; Current Methods in Inorganic Chemistry, vol. 1, Elsevier Science, Amsterdam, 1999, p. 355.